Performance Analysis of Multicarrier Code Select CDMA System for PAPR Reduction in Multipath Channels

Kwanwoong Ryu, Jiyu Jin, Yongwan Park, and Jeong-Hee Choi

Abstract: **Multicarrier direct sequence code division multiple access (MC DS-CDMA) is an attractive technique for achieving high data rate transmission. This is valid regardless of whether or not the potentially large peak-to-average power ratio (PAPR) is an important factor for its application. On the other hand, code select CDMA (CS-CDMA) is an attractive technique with constant amplitude transmission of multicode signal regardless of subchannels. This is achieved by introducing a code select method. In this paper, we propose a new multiple access scheme based on the combination of MC DS-CDMA and CS-CDMA. The proposed scheme, which we call MC CS-CDMA, includes as special cases the subclasses of MC DS-CDMA and CS-CDMA. This paper investigates the performance of these systems over a multipath frequency selective fading channel using a RAKE receiver with maximal ratio combiner. In addition, the PAPR of the proposed system is compared with that of both MC DS-CDMA and CS-CDMA. Simulation results demonstrate that the proposed system provides better PAPR reduction than MC DS-CDMA, at the expense of the complexity of the receiver and the number of available users. The numerical result demonstrates that the proposed system has better performance than MC DS-CDMA due to the increased processing gain and time diversity gain.**

Index Terms: **Code select method, multicarrier direct sequence code division multiple access (MC DS-CDMA), multicarrier CDMA, multicode CDMA, peak-to-average power ratio (PAPR).**

I. INTRODUCTION

Recently, multicarrier direct sequence code division multiple access (MC DS-CDMA) has been extensively studied for the fourth-generation (4G) wireless systems [1]–[11]. However, a main disadvantage of multicarrier CDMA is the high peak to average power ratio (PAPR) of the output signal, which may take values within a range that are proportional to the number of carriers in the system [11]–[17]. The high peak power in the transmitted signal will occasionally reach the amplifier saturation region and cause signal distortion, resulting in bit error rate (BER) degradation and spectral spreading. Generally, multicarrier CDMA is more sensitive to PAPR than single carrier CDMA because the number of subcarriers is increased. A scheme for reducing the PAPR should be utilized to reduce the high power amplifier (HPA) cost and increase HPA efficiency and battery life. To reduce the PAPR in OFDM, several proposals have been suggested and studied in the literature, such as clipping with filtering [12], block coding [13], partial transmit sequence [14], and selected mapping [15].

On the other hand, there have been studies on reducing the PAPR in multicarrier CDMA (MC-CDMA) [16]–[17]. Normally, the research for reducing the PAPR in parallel type signal processing has encompassed OFDM and MC-CDMA. However, the PAPR reduction scheme operates at the expense of BER performance. Furthermore, it is difficult to find solutions in the case of MC DS-CDMA because the symbol after serial-to-parallel (S/P) conversion is spread by spreading code. In this case, we have to consider simultaneously the parallel inter-symbol PAPR and inter-chip PAPR. Wada scheme [18] and code select CDMA (CS-CDMA) [19], [20] provide another way to reduce the PAPR for the multicode CDMA system. To avoid the large amplitude fluctuation in multicode CDMA, Wada scheme uses redundant bits. Compared to conventional multicode CDMA, this scheme can achieve a constant amplitude level of output signals. However, a disadvantage of this system is degraded transmission rate, by using parity check bits for constant amplitude coding. Also, the method described in [18] provided constant amplitude of output signals only if the spreading code sequence is the Hadamard code with special code length. Another interesting scheme is CS-CDMA. CS-CDMA has the advantage that it can easily achieve constant amplitude using a spreading code block (SCB), regardless of the kind of spreading code sequences. However, the disadvantages of this system are that transmission rate decreases and complexity of the receiver increases according to increasing in the number of subchannels [19], [20].

In this paper, we propose a new multicarrier CDMA system, called multicarrier code select CDMA (MC CS-CDMA). The proposed system has the following advantages: First, MC CS-CDMA is robust to the PAPR, because of the reduced number of subcarriers. Secondly, MC CS-CDMA can achieve better BER performance than MC DS-CDMA in situations with limited users. This paper is organized as follows: In Section II, we briefly review multicode CDMA with constant amplitude. In Section III, we introduce the proposed system, which includes a description of the transmitted signal, channel model and the receiver model. Section IV analyzes BER performance and Section V compares the proposed system with MC DS-CDMA. Finally, Section VI presents the conclusion.

II. MULTICODE CDMA WITH CONSTANT AMPLITUDE

The CS-CDMA can achieve constant amplitude transmission regardless of the number of input information bits [19], [20].

Manuscript received September 9, 2005; approved for publication by Lie-Liang Yang, Division II Editor, December 8, 2008.

K. Ryu is with the XRONet Corporation, Republic of Korea, email: kwryu@ynu.ac.kr.

J. Jin and Y. Park are with the Department of Information and Communication Engineering, Graduate school, Yeungnam University, Republic of Korea, email: {jyjin, ywpark}@ynu.ac.kr, corresponding author: Y. Park.

J.-H. Choi is with the School of Information and Communication Engineering, Daegu University, Republic of Korea, email: choijh@daegu.ac.kr.

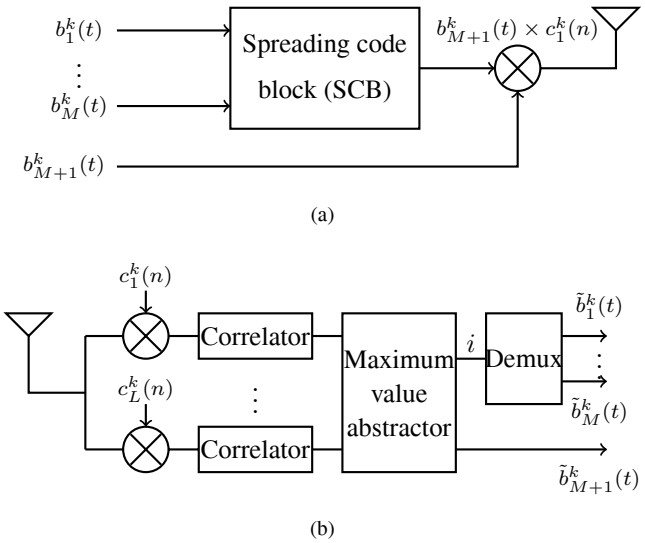

Fig. 1. Transmitter and receiver block diagram of CS-CDMA: (a) Transmitter and (b) receiver.

Fig. 1 shows the transceiver block diagram of CS-CDMA. The total number of branches are assumed as $(M+1)$ and the number of required code sequences of spreading code block (SCB) is assumed as 2^M. After S/P conversion, lth spreading code c_l^k of the SCB ($l = 1, 2, \cdots, 2^M$) is selected by input bits $(b_1^k, b_2^k, \cdots, b_M^k)$ of the kth user. These codes of the SCB can be periodic pseudo noise (PN) codes or orthogonal codes, and each of their chips belongs to the set $\{+1, -1\}$. After that, the symbol b_{M+1}^k is spread by the spreading code c_l^k. Therefore, the transmitted signal of user k can be expressed as

$$s_{CS}^k(t) = \sum_{l=-\infty}^{\infty} \sum_{n=1}^{N} b_{M+1}^k(i) c_l^k(n) p_c[t-(n-1)T_c - iT_s] \cdot \cos(2\pi f_0 t) \quad (1)$$

where $b_{M+1}^k(i)$ represents the last symbol of input symbols and N denotes the number of chips of the spreading code. The spreading sequence c_l^k represents the lth spreading code of user k in the SCB, it is selected by the ith input data sequence $(b_1^k, b_2^k, \cdots, b_M^k)$. In (1), T_s, T_c $(= T_s/N)$, and f_0 represent the symbol duration, the chip duration, and the carrier frequency of the CS-CDMA, respectively. The pulse waveform $p_c(t)$ is given by

$$P_c(t) = \begin{cases} 1, & 0 \le t \le T_s, \\ 0, & \text{otherwise.} \end{cases} \quad (2)$$

The received signal is despreaded by a set of code sequences in the SCB. The ith input sequence $\tilde{b}_1^k, \tilde{b}_2^k, \cdots, \tilde{b}_M^k$ is decided by the largest correlation value and $\tilde{b}_{M+1}^k$ is decided by the sign of the largest correlation value. The advantage of this scheme is that it achieves constant amplitude of output signals.

Table 1 shows the amplitude patterns of multicode CDMA and CS-CDMA. For fair comparison, we assume that the number of total input branches of both systems is the same: $P = M + 1$. In the case of $M = 3$ in CS-CDMA, 8 spreading codes are required.

Table 1. Output signal of multicode CDMA and CS-CDMA for 4 input data transmission ($M = 3$, total channels: $P = M + 1 = 4$).

	Input signal	Output signal	
		Multi-code CDMA	CS-CDMA
i	$(s_{i,0}, s_{i,1}, s_{i,2}, s_{i,3})$		(Spreading code) $\times\, b_{M+1}^k = c_l^k(n) \times b_4^k$
0	(0000)	-4,0,0,0	(W0) × 0=-1, -1, -1, -1, -1, -1, -1, -1
1	(0001)	-2,-2,-2,2	(W0) × 1=1, 1, 1, 1, 1, 1, 1, 1
2	(0010)	-2,2,-2,-2	(W1) × 0=1, -1, 1, -1, 1, -1, 1, -1
3	(0011)	0,0,-4,0	(W1) × 1=-1, 1, -1, 1, -1, 1, -1, 1
4	(0100)	-2,-2,-2,2	(W2) × 0=1, 1, -1, -1, 1, 1, -1, -1
5	(0101)	0,-4,0,0	(W2) × 1=-1, -1, 1, 1, -1, -1, 1, 1
6	(0110)	0,0,0,-4	(W3) × 0=1, -1, -1, 1, 1, -1, -1, 1
7	(0111)	2,-2,-2,-2	(W3) × 1=-1, 1, 1, -1, -1, 1, 1, -1
8	(1000)	-2,2,2,2	(W4) × 0=1, 1, 1, 1, -1, -1, -1, -1
9	(1001)	0,0,0,4	(W4) × 1=-1, -1, -1, -1, 1, 1, 1, 1
A	(1010)	0,4,0,0	(W5) × 0=1, -1, 1, -1, -1, 1, -1, 1
B	(1011)	2,2,-2,2	(W5) × 1=-1, 1, -1, 1, 1, -1, 1, -1
C	(1100)	0,0,4,0	(W6) × 0=1, 1, -1, -1, -1, -1, 1, 1
D	(1101)	2,-2,2,2	(W6) × 1=-1, -1, 1, 1, 1, 1, -1, -1
E	(1110)	2,2,2,-2	(W7) × 0=1, -1, -1, 1, -1, 1, 1, -1
F	(1111)	-4,0,0,0	(W7) × 1=-1, 1, 1, -1, 1, -1, -1, 1

Table 2. Comparison of systems ($P = M + 1$).

	Transmission data rate (R)	PAPR (dB)	♯ of required codes	The kind of code which can be available
Multi-code CDMA	R	$10 \log P$	P	All
Wada scheme	$3R/4$ (3/4 coding)	$P_{peak} = P_{ave} \to 0$	P	Hadamard code with special length
CS-CDMA	$PR/2^{P-1}$	$P_{peak} = P_{ave} \to 0$	2^{P-1}	All

As seen in Table 1, the sequence index number, which is 0, 3, 5, 6, 9, A, C, and F, of the input signal of multicode CDMA has a large amplitude. However, all output signals of the CS-CDMA have constant amplitude. Consequently, the CS-CDMA ensures the reduction of PAPR at the price of reduction of transmission data rate, compared to that of multicode CDMA.

Table 2 shows the characteristics of three schemes; namely, the multicode CDMA system, the Wada scheme [18], and CS-CDMA in terms of the transmission data rate, PAPR, the number of the required codes and the type of code sequence available. The Wada scheme and CS-CDMA dramatically reduce the PAPR compared with multicode CDMA. In contrast to the CS-CDMA system, the Wada scheme provided constant amplitude of output signals with the use of the Hadamard code with special length. However, the complexity of the CS-CDMA receiver is higher than that of multicode CDMA. The transmission data rate also decreases as the number of subchannels, P, increases.

III. MC CS-CDMA SYSTEM

A. Transmitted Signal

Our design target focuses on improved time diversity gain and PAPR reduction at the expense of receiver complexity in pure MC DS-CDMA [5], [10]. To achieve this purpose, we consider a combination of MC DS-CDMA and CS-CDMA. The reason for selecting CS-CDMA instead of the Wada scheme is that the Wada scheme can be used only with a Hadamard code of special length. We shall refer to the proposed scheme as MC CS-CDMA, as shown in Fig. 2. Fig. 2 shows the kth user's transmitter schematic of the MC CS-CDMA system. At the transmitter

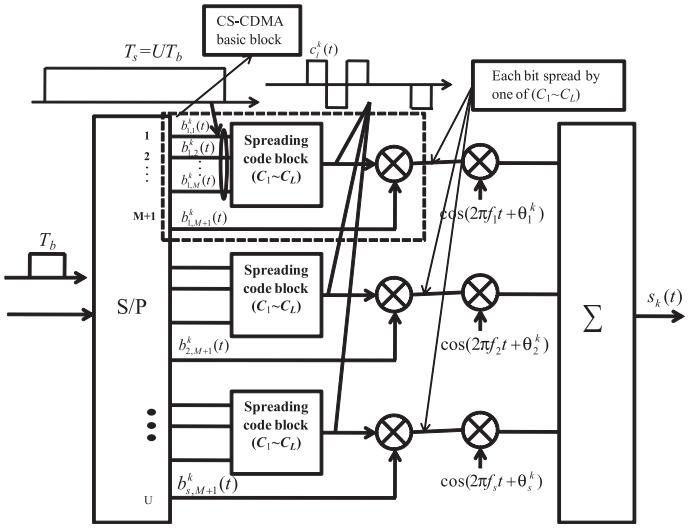

Fig. 2. The kth user's transmitter schematic for MC CS-CDMA.

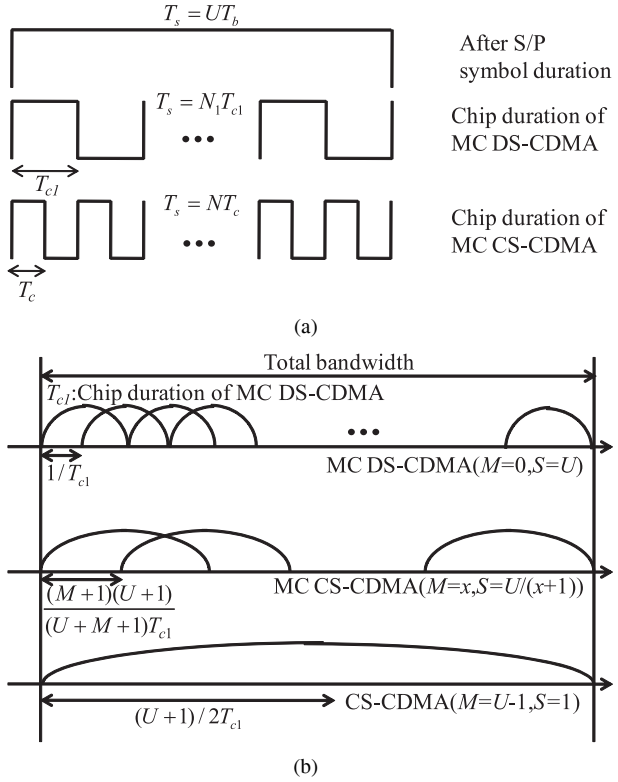

Fig. 3. Time and frequency domain signals of MC DS-CDMA and MC CS-CDMA system: (a) Chip duration of MC DS-CDMA and MC CS-CDMA, and (b) spectrum of MC DS-CDMA and MC CS-CDMA.

side, the binary bit stream is S/P converted to U parallel substreams. The bit duration or symbol duration of each substream is $T_s = UT_b$, M represents the number of input bits per SCB, and $S = U/(M+1)$ represents the number of groups or the number of subcarriers. A selected spreading code out of SCB multiplies with the $(M+1)$th bit and then modulated by a subcarrier. Transmitted signals of user k consist of summations of signals of these groups. Therefore, the transmitted signal of user k can be expressed as

$$s_k(t) = \sqrt{2P}\sum_{s=1}^{S} b^k_{s,(M+1)}(t)c^k_{s,l}(t)\cos(2\pi f_s t + \theta^k_s), \quad l = 1,\cdots,L \tag{3}$$

where P represents the transmitted power per subcarrier. $\{b^k_{s,(M+1)}(t)\}$, $\{c^k_{s,l}(t)\}$, and $\{f_s\}$ represent each group's $(M+1)$th bit waveform, spreading code waveform, and subcarrier frequency of the sth group of the kth user, respectively. We assume that phase θ^k_s represents the initial phase of the sth subcarrier of the kth user. The $(M+1)$th data sequence is defined as

$$b^k_{s,(M+1)}(t) = \sum_{i=-\infty}^{\infty} b^k_{s,(M+1)} P_{T_s}(t - iT_s) \tag{4}$$

where $b^k_{s,(M+1)}$ is a rectangular pulse waveform which is defined as the interval $[0, T_s)$ and assumes values of +1 and -1 with equal probability. In (4) and (5), P_{T_s} and P_{T_c} represent the impulse shaping of data sequence and spreading sequence, respectively. kth user's spreading code sequence of SCB is expressed as

$$c^k_{s,l}(t) = \sum_{j=-\infty}^{\infty} c^k_{s,l,j} P_{T_c}(t - jT_c) \tag{5}$$

where $c^k_{s,l,j}$ also assumes values of $+1$ and -1 with equal probability. The spacing between two adjacent subcarrier frequencies is assumed as $1/T_c$. Here, T_c represents the chip duration of MC CS-CDMA. If the processing gain of MC CS-CDMA is N, it can be expressed as $T_c = T_s/N$. Therefore, the orthogonal frequency of the subcarrier is represented as

$$f_s = f_c + (s-1)\frac{1}{T_c}, \quad s = 1,2,\cdots,S \tag{6}$$

where f_c represents center frequency, s represents the subcarrier index. The bandwidth and the data rate of the MC CS-CDMA is the same as the CS-CDMA. Fig. 3 shows the characteristics of MC DS-CDMA and MC CS-CDMA in the time and frequency domain. Fig. 3(a) shows the time domain signal of MC DS-CDMA and MC CS-CDMA after S/P conversion. Let $T_{c1} = T_s/N_1$ be the chip duration of MC DS-CDMA and $T_c = T_s/N$ be the chip duration of MC CS-CDMA. Fig. 3(b) shows the frequency domain signal of both systems. We assume that the subcarrier spacing of MC DS-CDMA and MC CS-CDMA are $\Delta f_{MC-DS} = 1/T_{c1}$ and $\Delta f_{MC-CS} = 1/T_c$, respectively. Also, U represents the total number of branches. We use the total spectrum of the MC DS-CDMA $W_{MC-DS} = (U+1)/T_{c1}$ as a reference spectrum in this paper. To make a fair comparison between the performance, as shown in Fig. 3(b), we create the same total bandwidth of MC CS-CDMA using variable parameters M and S as that of MC DS-CDMA. With an increase in the number of input symbol M, the number of total subcarrier decreases. Therefore, we obtain the total number of subcarriers as $U/(M+1)$ and the total spectrum of MC CS-CDMA as $W_{MC-CS} = (U/(M+1)+1)(1/T_c)$. Assuming that the total bandwidth of both systems are the same, we can define the

relationship of the chip duration of both systems as follows:

$$T_c = \frac{U+M+1}{(M+1)(U+1)} T_{c1}. \tag{7}$$

We conclude that the chip duration of MC CS-CDMA decreases according to increasing M value under fixed total bandwidth. Each subcarrier bandwidth and spreading gain of MC CS-CDMA increases according to decreasing the number of subcarrier of MC CS-CDMA. If $M = 0$, MC CS-CDMA belongs to MC DS-CDMA. However, if $M = U - 1$, MC CS-CDMA belongs to CS-CDMA where U is the number of parallel sub-streams after S/P. Therefore, both MC DS-CDMA and CS-CDMA can be considered as members of MC CS-CDMA systems with arbitrary code selection of $M \in \{0, \cdots, U-1\}$. The input index M in MC CS-CDMA can be adjusted. If M is high, for example $M = U - 1$, in the context of CS-CDMA, given total bandwidth and high value of M, a high spreading gain can be maintained, which leads to the reduction of multiuser interference and the PAPR. Therefore, the highest possible diversity gain is achieved since the resolvable path is increased in the propagation environment encountered. However, the complexity of the receiver increases. By contrast, if M is low, for example, $M = 0$, in the context of MC DS-CDMA, the spreading of each subcarrier signal is low, which leads to increased multiuser interference and PAPR and small diversity gain.

B. Channel Model

Total subcarrier signal having equal received power exponentially decaying multipath intensity profile (MIP) distribution for l_pth multipath component of the channel can be expressed as

$$\Omega^k_{s,l_p} = \Omega^k_0 e^{-\eta l_p}. \tag{8}$$

This functional form for Ω^k_{s,l_p} accounts for the decay of average path length as a function of path decay. Ω^k_0 is the first resolvable path of average signal strength and η is average power attenuation rate. If we assume the receiver of all users have perfect power control, (8) is represented as $\Omega^k_{s,l_p} = \Omega_0 e^{-\eta l_p}$. If we consider the number of L_p paths signals (8) can be expressed as

$$\sum_{l_p=0}^{L_p-1} \Omega^k_{s,l_p} = \sum_{l_p=0}^{L_p-1} \Omega^1_{s,l_p} = \Omega_0 q(L_p, \eta) \tag{9}$$

where

$$\begin{aligned} q(L_p,\eta) &= \sum_{l_p=0}^{L_p-1} e^{-\eta l_p} \\ &= \begin{cases} (1-e^{-\eta L_p})/(1-e^{-\eta}), & \eta \neq 0, \\ L_p, & \eta = 0. \end{cases} \end{aligned} \tag{10}$$

Finally, the average multipath signal Ω^k_{s,l_p} can be expressed as $q(L_p,\eta)\Omega_0/L_p$. Meanwhile, we consider the number of paths between MC CS-CDMA and MC DS-CDMA. We assume the maximum delay spread of the communication channel is defined as $T_m \approx 1/(\triangle f_c)$. Then the number of resolvable paths,

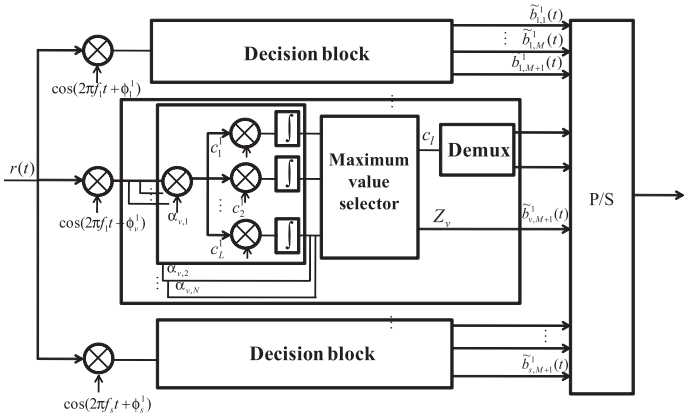

Fig. 4. Receiver block diagram of MC CS-CDMA system.

L_{MC-CS}, associated with the MC CS-CDMA signal is given by $L_{MC-CS} = \lfloor T_m/T_c \rfloor + 1$, where $\lfloor x \rfloor$ represents the largest integer not exceeding x. The number of resolvable paths, L_{MC-DS}, in the context of the corresponding MC DS-CDMA signal is given by $L_{MC-DS} = \lfloor T_m/T_{c1} \rfloor + 1$. Multiply both sides of the inverse of (7) by T_m, we obtain that L_{MC-CS} and L_{MC-DS} are related by

$$L_{MC-CS} \approx \left\lfloor \frac{(M+1)(U+1)}{U+M+1} (L_{MC-DS} - 1) \right\rfloor + 1. \tag{11}$$

We express L_{MC-DS} and L_{MC-CS} as L_p in the next section.

C. Receiver

Fig. 4 shows the receiver of MC CS-CDMA using maximal ratio combining (MRC) equalizer and RAKE receiver for diversity gain. We assume the receiver is capable of acquiring perfect time-domain synchronization with each path of the reference signal. The multipath attenuations and phases are assumed to be perfect estimates of channel parameters. MC CS-CDMA and MC DS-CDMA can be considered as the same type system with spreading after parallel data transmission. Therefore, we can extend the BER performance of MC DS-CDMA in multipath Rayleigh fading for analyzing that of MC CS-CDMA. The transmitted signal $s_k(t)$, which passes the radio channel attenuated by multipath fading and AWGN can be written as

$$\begin{aligned} r(t) =& \sqrt{2P} \sum_{k=1}^{K} \sum_{s=1}^{S} \sum_{l_p=0}^{L_p-1} \alpha^k_{s,l_p} b^k_{s,(M+1)}(t-\tau^k_{lp}) c^k_{s,l}(t-\tau^k_{lp}) \\ & \cdot \cos(2\pi f_s t + \phi^k_{s,l_p}) + n(t) \end{aligned} \tag{12}$$

where α^k_{s,l_p}, $\tau^k_{l_p}$, and $\phi^k_{s,l_p} = \theta^k_s - \beta^k_{s,l_p} - 2\pi f_s \tau^k_{l_p}$ represent the kth user's attenuation factor, delay and phase-shift for the l_pth multipath component of the channel, respectively. ϕ^k_{s,l_p} and α^k_{s,l_p} are independent identically distributed (i.i.d) random variables uniformly distributed in the interval $[0, 2\pi)$ and multipath Rayleigh fading distribution. $n(t)$ is the additive white gaussian noise with zero mean and double-sided power spectral density $N_0/2$. The received signal of vth subcarrier correlates with the number of received matched filters, L, and decides Z_v and Γ_l.

The $(M+1)$th symbol of kth user's vth subcarrier, Z_v, is decided as

$$\begin{cases} b^k_{v,M+1} = 1, & \text{if } Z_v > 0, \\ b^k_{v,M+1} = -1, & \text{if } Z_v \le 0. \end{cases} \tag{13}$$

On the other hand, the probability of $(b^k_{v,1}, b^k_{v,2}, \cdots, b^k_{v,M})$, C_l, is decided as

$$C_l = index[\max(|d_l|)], \quad l = 1, \cdots, L \tag{14}$$

where $d_l = \int_0^T r(t) \sum_{n=1}^{N} \alpha_{v,n} \sum_{l=1}^{L} C^s_{v,l} dt$ represents the correlation value of received signal ($index[d_l] \in \{C_1, C_2, \cdots, C_L\}$) and C_l represents the maximum l spreading code, which has a maximum correlation value of SCB. Finally, the U numbers of parallel data are parallel-to-serial (P/S) converted, in order to output the serial data bits.

IV. PERFORMANCE ANALYSIS

We detect the number of M symbols using the detection information of $(M+1)$th symbol, after detecting $(M+1)$th symbol. Therefore, we assume that the BER of the number of M symbols is approximately same as that of $(M+1)$th symbol in this paper. We analyze the statistics of the decision variable. After MRC is conducted, the output of the reference user of matched filter of vth subcarrier and nth path can be expressed as

$$Z_{v,n} = \int_{\tau_n}^{T_s+\tau_n} r(t) \alpha_{v,n} c^k_{v,l}(t - \tau^k_n) \cos(2\pi f_v t + \phi^k_{v,n}) dt. \tag{15}$$

Without loss of generality, we set $\tau^k_n = 0$ and $\phi^k_{v,n} = 0$ of (15) for analyzing the statistics of the decision variable Z_v. We assume the decision variable Z_v consists of λ fingers of the RAKE receiver. Therefore, for the decision static based on the decision variable of the vth subcarrier Z_v, $v = 1, 2, \cdots, D$ expressed as

$$Z_v = \sum_{n=0}^{\lambda-1} Z_{v,n}, \qquad v = 1, 2, \cdots, D. \tag{16}$$

The vth subcarrier consists of the parallel combination of λ RAKE fingers ($1 < \lambda < L_p$) and it's λ'th finger is assumed to be synchronized with the l_pth path among the L_p resolvable paths of the reference user. The normalized mean of Z_v is given by

$$E[Z_v] = E[D] = \sqrt{\frac{P}{2}} T_s b^1_{v,(M+1)} \sum_{n=0}^{\lambda-1} (\alpha^1_{v,n})^2. \tag{17}$$

The mean of channel noise is zero and the variance of channel noise is expressed as

$$var(\eta) = \frac{N_0 T_s}{4} \sum_{n=0}^{\lambda-1} (\alpha^1_{v,n})^2. \tag{18}$$

The variance of interference is expressed as

$$\begin{aligned} var[I] =& \frac{P}{2} T_s^2 \Bigg[\frac{1}{3N} \left((L_p - 1) E\{(\alpha^1_{v,l_p})^2\} \right) + (K-1) \\ & \cdot L_p E\{(\alpha^k_{v,l_p})^2\} + (S-1) \bar{I} (L_p - 1) E\{(\alpha^1_{v,l_p})^2\} \\ & + (K-1) L_p E\{(\alpha^1_{v,l_p})^2\} \Bigg] \sum_{n=0}^{\lambda} (\alpha^1_{v,n})^2. \end{aligned} \tag{19}$$

Consequently, the variance of the total decision variable is represented as

$$\begin{aligned} var[Z_v] =& \sum_{n=0}^{\lambda-1} [Z_{v,n}] \\ =& \frac{P}{2} T_s^2 \Bigg[\frac{N_0}{2E_b \Omega_0} + \frac{1}{3N} (KL_p - 1) \frac{q(L_p, \eta)}{L_p} \\ & + (S-1) \bar{I} (KL_p - 1) \frac{q(L_p, \eta)}{L_p} \Bigg] \Omega_0 \sum_{n=0}^{\lambda-1} (\alpha^1_{v,n})^2. \end{aligned} \tag{20}$$

In (20), the mean of the same term ($\bar{I}$) can be expressed as

$$\begin{aligned} \bar{I} =& \frac{1}{D(D-1)} \sum_{v=1}^{D} \sum_{d=1, d \ne v}^{D} \frac{1}{2\pi^2 (d-v)^2 N} \\ & \cdot \{1 - \text{sinc}(2\pi(d-v))\}. \end{aligned} \tag{21}$$

Using (16) in [3], the mean of the same term ($\bar{I}$) can be expressed as

$$\begin{aligned} \bar{I} =& \frac{1}{D(D-1)} \sum_{v=1}^{D-1} \sum_{d=v+1}^{D} \frac{1}{\pi^2 (d-v)^2 N} \\ & \cdot \{1 - \text{sinc}(2\pi(d-v))\}. \end{aligned} \tag{22}$$

The decision variable Z_v assumes the Gaussian random variable with the mean is (17) and the variance is (20). Generally, the conditional BER of the fading parameter α is expressed as (23) [10]

$$P_b = Q\left(\sqrt{\frac{(E[Z_v])^2}{Var(Z_v)}} \right) = Q\left(\sqrt{2 \sum_{n=0}^{\lambda-1} \gamma_n} \right) \tag{23}$$

where

$$\gamma_n = \frac{(\alpha^1_{s,l_p})^2}{\Omega_0} \gamma_c \tag{24}$$

and $Q(\cdot)$ is defined as follows:

$$Q(x) = \frac{1}{\sqrt{2\pi}} \int_x^{\infty} e^{-t^2/2} dt. \tag{25}$$

The alternative representation was proposed by Graig who showed that the Gaussian $Q(\cdot)$-function (25) expressed as (26) in the following definite integral form [22] is

$$Q(x) = \frac{1}{\pi} \int_0^{\pi/2} \exp\left(-\frac{x^2}{2\sin^2\theta} \right) d\theta, \qquad x \ge 0. \tag{26}$$

If the random variables $\{\gamma_l\}_{n=0}^{\lambda-1}$ are assumed to be statistically independent in a multipath channel environment, we have $P_{\gamma_0,\gamma_1,\cdots,\gamma_{\lambda-1}}(\gamma_0,\gamma_1,\cdots,\gamma_{\lambda-1}) = \prod_{n=0}^{\lambda-1} p_{\gamma_n}(\gamma_n)$ and the average BER can be expressed as [22]

$$\begin{aligned} P_b(E) &= \int_0^\infty \int_0^\infty \cdots \int_0^\infty P_b(\{\gamma_{n=0}^{\lambda-1}\}) \\ &\quad \cdot \prod_{n=0}^{\lambda-1} p_{\gamma_l}(\gamma_\lambda) d_{\gamma_0} d_{\gamma_1} \cdots d_{\gamma_{\lambda-1}} \\ &= \underbrace{\int_0^\infty \int_0^\infty \cdots \int_0^\infty}_{\lambda-fold} \frac{1}{\pi} \int_0^{\pi/2} \\ &\quad \cdot \prod_{n=0}^{\lambda-1} \exp(-\frac{g\gamma_\lambda}{\sin^2\phi}) p_{\gamma_\lambda}(\gamma_\lambda) d_{\gamma_0} d_{\gamma_1} \cdots d_{\gamma_{\lambda-1}} \end{aligned} \quad (27)$$

where $g = 1$ for coherent binary-shift keying (BPSK), $g = 1/2$ for coherent orthogonal binary frequency shift keying (BFSK) and $g = 0.715$ for coherent BFSK with minimum correlation. In the BPSK system, we can express this as the following [10], [22]

$$\begin{aligned} P_b(E) &= \int_0^\infty \int_0^\infty \cdots \int_0^\infty Q\left(\sqrt{\frac{\sum_{n=0}^{\lambda-1}\gamma_n}{\sin^2\theta}}\right) \\ &\quad \cdot \prod_{n=0}^{\lambda-1} p_{\gamma_n}(\gamma_n) d_{\gamma_0} d_{\gamma_1} \cdots d_{\gamma_{\lambda-1}}. \end{aligned} \quad (28)$$

Finally, the average BER for generalized MC CS-CDMA can be expressed as [10]

$$P_b(E) = \frac{1}{\pi} \int_0^{\pi/2} \prod_{n=0}^{\lambda-1} (\frac{m\sin^2\theta}{\bar{\gamma}_n + m\sin^2\theta})^m d\theta \quad (29)$$

where $\bar{\gamma}_n = \gamma_c e^{-\eta n}$ for $n = 0, 1, \cdots, \lambda-1$ and

$$\begin{aligned} \gamma_c &= \Bigg[\left(\frac{\Omega_0 E_b}{N_0}\right)^{-1} + \frac{2}{3N}[(L_p-1)E\{(\alpha_{v,l_p}^1)^2\} + (K-1) \\ &\quad \cdot L_p E\{(\alpha_{v,l_p}^k)^2\}] + 2(S-1)\bar{I}(L_p-1)E\{(\alpha_{v,l_p}^1)^2\} \\ &\quad + (K-1)L_p E\{(\alpha_{v,l_p}^1)^2\} \Bigg]^{-1} \\ &= \Bigg[\left(\frac{\Omega_0 E_b}{N_0}\right)^{-1} + \frac{2}{3N}(KL_p-1)\frac{q(L_p,\eta)}{L_p} + 2(S-1) \\ &\quad \cdot \bar{I}(KL_p-1)\frac{q(L_p,\eta)}{L_p} \Bigg]^{-1} \\ &= \Bigg[\left(\frac{\Omega_0 E_b}{N_0}\right)^{-1} + 2(KL_p-1)\frac{q(L_p,\eta)}{L_p} \\ &\quad \cdot \left(\frac{1}{3N} + (S-1)\bar{I}\right) \Bigg]^{-1}. \end{aligned} \quad (30)$$

When $\eta = 0$, each path has the same MIP distribution in (29). Therefore, $\{\gamma_n\}_{n=0}^{\lambda-1}$ in (27) are i.i.d. random variables and $\bar{\gamma}_0 = \bar{\gamma}_1 = \cdots = \bar{\gamma}_{\lambda-1} = \gamma_c$. When m is 1, the Nakagami fading channel model of (31) is expressed as a Rayleigh fading model in multipath fading. Therefore, when $\eta = 0$ and $m = 1$, (29) is easily expressed as

$$P_b(E) = \left[\frac{1-\mu}{2}\right]^\lambda \sum_{n=0}^{\lambda-1} \binom{L-1+n}{n} \left[\frac{1+\mu}{2}\right]^n \quad (31)$$

where $\mu = \sqrt{\gamma_c/(\gamma_c+1)}$. Then, (31) represents the average BER of BPSK modulation over multipath Rayleigh fading [21].

Table 3. Major parameters.

	MC DS-CDMA	MC CS-CDMA					CS-CDMA
	$M=0$ $D=60$	$M=1$ $D=30$	$M=2$ $D=20$	$M=3$ $D=15$	$M=4$ $D=12$	$M=5$ $D=10$	M=U=1 $S=1$
Chip duration (T_{c1})	1	0.508	0.344	0.262	0.213	0.18	0.03
Spreading gain	127	249	368	483	595	704	3873
Number of users	127	325	92	60	37	23	1
Number of path (power/path)	1 (1)	2 (1/2)	2 (1/2)	2 (1/2)	3 (1/3)	4 (1/4)	34 (1/34)

V. NUMERICAL RESULTS AND SIMULATION RESULTS

In this section, we evaluate the performance of MC CS-CDMA and compare it with that of MC DS-CDMA and CS-CDMA. For convenience, the parameters of MC CS-CDMA corresponding to MC DS-CDMA system are summarized as Table 3. The total number of branches is $U = 60$ and the overall bandwidth and data rate are the same. The comparison is based on the uniform MIP channel condition with $T_m = 0.508T_{c1}$. Also, we assume that path timing detection for path searching and channel estimation are perfect. When we assume MC DS-CDMA as reference, the chip duration, the spreading gain, and the number of resolvable path of MC DS-CDMA are $T_{c1} = 1$, $N_1 = 127$, and $L_{MC-DS} = 1$, respectively. The number of resolvable paths of both systems is computed from (11). To make equal power, the power of both systems per path represents 1/(the number of total paths). In addition, the number of available users are computed from (spreading gain)/(the number of required spreading code per user) as shown in Table 3. As we mentioned before, it is shown that as the number of subcarriers increases, the bandwidth on each subcarrier is reduced and it is subject to less resolvable multipath. With sufficient number of carriers such as MC DS-CDMA, the condition of single-path fading for each subcarrier is achieved. From the results of Figs. 5 and 6, we observe the performance of CS-CDMA, MC DS-CDMA, and MC CS-CDMA.

In Fig. 5, the analytical expression and the simulation results of CS-CDMA, MC DS-CDMA, and MC CS-CDMA are compared when the number of users are one. The plot shows that analytical derivations agree closely with the simulation results. We assumed that all resolvable paths are combined in the receiver irrespective of the complexity. In the same delay spread, the number of multipath of CS-CDMA is larger than the other scheme as shown in Table 3. Therefore, it is possible to achieve a larger time diversity gain than with the other schemes. As well, the MC CS-CDMA system has better performance than

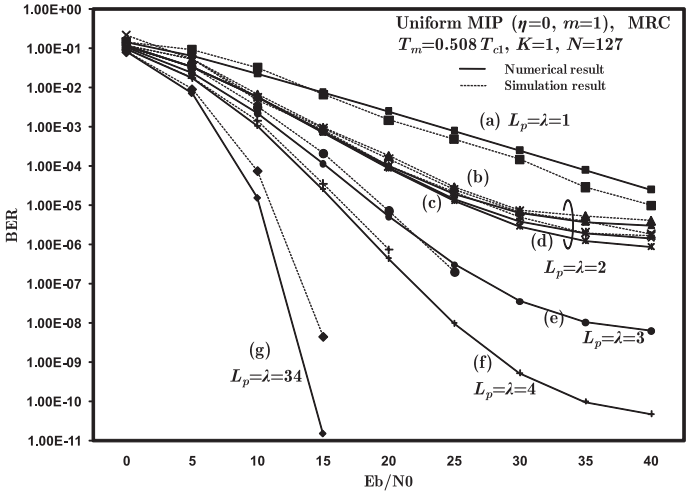

Fig. 5. BER performance of MC DS-CDMA in multipath Rayleigh fading: $N = 127$, $\eta = 0$, $m = 1$, $K = 1$; MC DS-CDMA: (a) $S = 60$; MC CS-CDMA: (b) $M = 1$, $S = 30$, (c) $M = 2$, $S = 20$, (d) $M = 3$, $S = 15$, (e) $M = 4$, $S = 12$, and (f) $M = 5$, $S = 10$; CS-CDMA: (g) $M = 0$, $S = 1$.

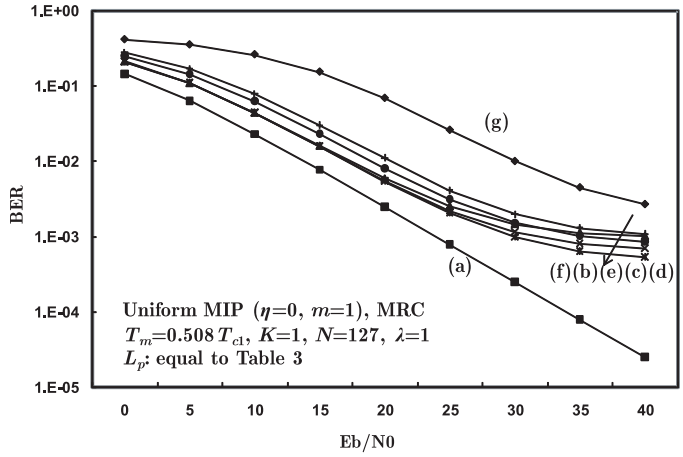

Fig. 6. BER performance of MC DS-CDMA and MC CS-CDMA in multipath Rayleigh fading: $N = 127$, $\eta = 0$, $m = 1$, $K = 10$; MC DS-CDMA: (a) $S = 60$; MC CS-CDMA: (b) $M = 1$, $S = 30$, (c) $M = 2$, $S = 20$, (d) $M = 3$, $S = 15$, (e) $M = 4$, $S = 12$, and (f) $M = 5$, $S = 10$; CS-CDMA: (g) $M = 0$, $S = 1$.

does MC DS-CDMA for the same reason. In high $Eb/N0$, the performance of MC CS-CDMA becomes saturated since the effect of multipath interference (MPI) increases as the number of multipaths increases. However, the CS-CDMA system does not saturate since the diversity gain can sufficiently reduce the effect of MPI. One of the disadvantages as M increases is that the number of available users decreases. For example, the number of available users is only a single user in the CS-CDMA system. Fig. 6 shows the performance of CS-CDMA, MC DS-CDMA, and MC CS-CDMA when the number of the fingers of RAKE receiver is one, where the other parameters are the same as in Fig. 5.

The MC DS-CDMA outperforms other schemes. As M increases, the performance is degraded due to an increasing loss of energy of the received signal as limited the number of finger of RAKE receiver. Therefore, the CS-CDMA becomes the worst performer.

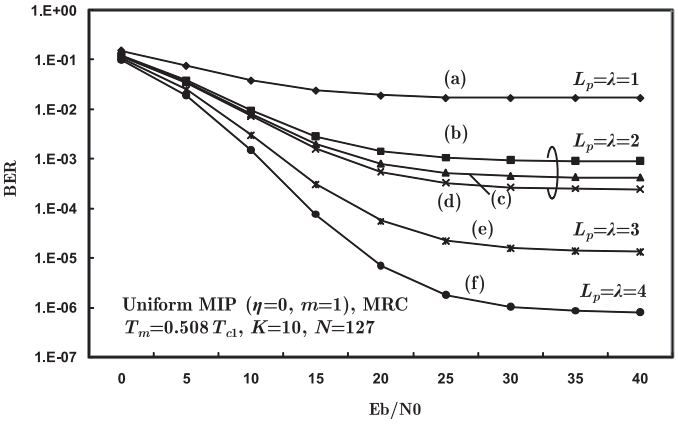

Fig. 7. BER performance of MC DS-CDMA and MC CS-CDMA in multipath Rayleigh fading: $N = 127$, $\eta = 0$, $m = 1$, $K = 10$; MC DS-CDMA: (a) $S = 60$; MC CS-CDMA: (b) $M = 1$, $S = 30$ (c) $M = 2$, $S = 20$, (d) $M = 3$, $S = 15$, (e) $M = 4$, $S = 12$, and (f) $M = 5, S = 10$.

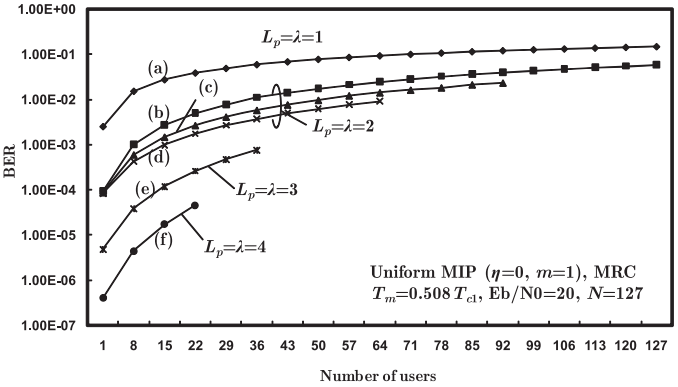

Fig. 8. BER performance of MC DS-CDMA and MC CS-CDMA in multipath Rayleigh fading and $Eb/N0 = 20$ dB, $N = 127$, $\eta = 0$, $m = 1$ BER vs. users in MC DS-CDMA: (a) $S = 60$; MC CS-CDMA: (b) $M = 1$, $S = 30$, (c) $M = 2$, $S = 20$, (d) $M = 3$, $S = 15$, (e) $M = 4$, $S = 12$, and (f) $M = 5$, $S = 10$.

In Fig. 7, the BER versus the performance of MC CS-CDMA and MC DS-CDMA was evaluated when the number of users is ten. We can not consider CS-CDMA in this figure since that system accommodates only one user. The MC CS-CDMA outperforms MC DS-CDMA. The interpretation for the above observation is as follows: When Mincreases in MC CS-CDMA: 1) The performance of this system improves since the time diversity increases even if each power per path decreases as the number of multipaths increases. 2) The processing gain of this system increases so that the effect of multiuser interference reduces.

In Fig. 8, we evaluated the BER versus the number of available users in the context of MC DS-CDMA and MC CS-CDMA at $Eb/N0 = 20$ dB, where the parameters are the same as in Fig. 7. It can be seen that MC CS-CDMA outperforms the MC DS-CDMA in the environment of limited users. Also, the MC CS-CDMA with $M = 1$, $M = 2$, and $M = 3$ has the same diversity gain, but $M = 3$ has better performance than other cases

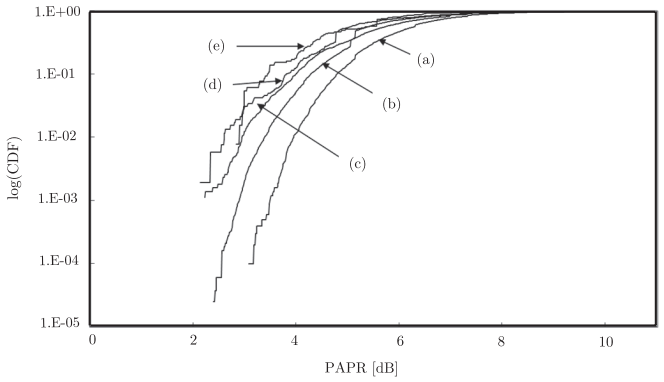

Fig. 9. PAPR CDF of MC CS-CDMA and MC DS-CDMA ($U = 60$), MC DS-CDMA: (a) $S = 60$; MC CS-CDMA: (b) $M = 2,\ S = 20$, (c) $M = 3,\ S = 15$, (d) $M = 4,\ S = 12$, and (e) $M = 5,\ S = 10$.

Table 4. Comparison to complexity per each subcarrier of three schemes in receiver ($T_m = 0.508T_{c1}$).

	MC DS-CDMA	MC CS-CDMA					CS-CDMA
	$M = 0$ $S = 60$	$M = 1$ $S = 30$	$M = 2$ $S = 20$	$M = 3$ $S = 15$	$M = 4$ $S = 12$	$M = 5$ $S = 10$	$M = 59$ $S = 1$
λ	1	2	2	2	3	4	34
L	1	2	4	8	16	32	2^{59}

due to higher processing gain. Therefore, we can conclude that MC CS-CDMA alleviates the effect of multiuser interference (MUI), when increasing M value with limited user. However, the MC DS-CDMA can accommodate larger available user than other schemes.

Fig. 9 shows cumulative distribution functions (CDFs) of PAPR in MC DS-CDMA and MC CS-CDMA with M. As well, it can be seen from this figure that according to M, the MC CS-CDMA systems have lower PAPR than MC DS-CDMA. In PAPR of 4 dB, the number of symbols under 4 dB are (a) 0.0125 (1.25%), (b) 0.053 (5.3%), (c) 0.116 (11.6%), (d) 0.14 (14%), and (e) 0.18 (18%), respectively. This is because the number of subcarrier (S) decreases as M increases. The CS-CDMA has the best PAPR since the peak power and average power of this system are the same. The key issue in designing a receiver of MC DS-CDMA, CS-CDMA and MC CS-CDMA is its complexity.

Table 4 shows that the receiver complexity of three schemes per each subcarrier in terms of the number of fingers of the RAKE receiver is λ and the number of correlators of SCB is L. The receiver of CS-CDMA has the highest complexity and MC DS-CDMA has the lowest complexity. For full recovery of all considered multipath components, the CS-CDMA System requires a RAKE receiver with a large number of fingers, in order to capture the majority of available energy. However, combining many paths using a RAKE receiver significantly increases the complexity of the implementation. There is a trade-off between RAKE Receiver complexity and its performance.

Consequently, there is a need to design an MC CS-CDMA that has a reasonable number of fingers, in terms of cost, and that also has an ability to collect the majority of the available energy from multipath channel. In the numerical results, the CS-CDMA has the best performance over the other schemes assuming the path timing detection for path searching and channel estimation are perfect. However, the performance of the CS-CDMA is severely degraded due to increasing errors in path timing detection for path searching and channel estimation caused by severe MPI in practical environment. Also, the complexity of receiver of CS-CDMA becomes very high. We concluded that the CS-CDMA is not practical in the same transmission rate and bandwidth as MC DS-CDMA. Therefore, our conclusion is that we may carefully assign the number of M of MC CS-CDMA, depending on the quality of service required such as PAPR, system complexity, and channel environment in a practical environment.

VI. CONCLUSIONS

The proposed MC CS-CDMA system belongs to a multicarrier CDMA system, which is a combination of MC DS-CDMA and CS-CDMA schemes. The numerical results show that, in the same bandwidth and transmission data rate with MC DS-CDMA, MC CS-CDMA is robust with respect to multiuser interference due to increasing spreading gain and diversity gain. We also investigated the PAPR of both systems. The results show that MC CS-CDMA reduced PAPR compared to MC DS-CDMA. However, the advantages of MC CS-CDMA were gained at the expense of higher system complexity of the receiver when increasing various parallel input bits (M) of SCB and the number of fingers of RAKE receiver in each subcarrier. Also, the number of available users decreased according to increasing M. Due to the PAPR reduction, the bandwidth efficiency and the system complexity of MC CS-CDMA have some degree of compatibility, and we may assign the number of M depending on the quality of service required.

ACKNOWLEDGMENTS

The authors are very grateful to the anonymous reviewers for their useful comments.

REFERENCES

[1] L.-C. Wang and C.-W. Chang, "On the performance of multicarrier DS-CDMA with imperfect power control and variable spreading factors," *IEEE J. Sel. Areas Commun.*, vol. 24, no. 6, pp. 1154–1166, June 2006.

[2] J. Jin, K.-W. Ryu, and Y. Park, "A full rate quasi-orthogonal STF-OFDM with DAC-ZF decoder over wireless fading channels," *ETRI J.*, vol. 28, no. 1, pp. 87–90, Feb. 2006.

[3] E. A. Sourour and M. Nakagawa, "Performance of orthogonal multicarrier CDMA in a multipath fading channel," *IEEE Trans. Commun.*, vol. 44, pp. 356–366, Mar. 1996.

[4] A. M. Tulino, L. Li, and S. Verdú, "Spectral efficiency of multicarrier CDMA," *IEEE Trans. Inf. Theory*, vol. 51, no. 2, pp. 479–505, Feb. 2005.

[5] S. Elnoubi and A. El Beheiry, "Effect of overlapping between successive carriers of multi-carrier CDMA on the performance in a multi-path fading channel," *IEEE Trans. Commun.*, vol. 49, pp. 769–773, May 2001.

[6] R. Prasad, *Universal Wireless Personal Communications*. Artech, 1998.

[7] R. Prasad and S. Hara, "Overview of multicarrier CDMA," *IEEE Commun. Mag.*, pp. 126–133, Dec. 1997.

[8] N. Yee, J.-P. Linnartz, and G. Fettweis, "Multi-carrier CDMA in indoor wireless radio networks," in *Proc. IEEE PIMRC*, Sept. 1993, pp. 109–113.

[9] K.-W. Ryu, Y. Kishiyama, and Y. Park, "Investigation of STBC and TSTD transmitter diversity effect using Chase combining in spread OFDM broadband packet wireless access," *IEICE Trans. Commun*, vol. E89-B, no. 5, pp. 1700–1704, May 2006.

[10] L.-L. Yang and L. Hanzo, "Performance of generalized multicarrier DS-CDMA over Nakagami-m fading channels," *IEEE Trans. Commun.*, vol. 50, no. 6, pp. 956–966, June 2002.
[11] S. Han and J. Lee, "An overview of peak-to-average power ratio reduction techniques for multicarrier transmission," *IEEE Wireless Commun.*, vol. 12, no. 2, pp. 56–64, Apr. 2005.
[12] L. Xiaodong and L. J. Cimini Jr., "Effects of clipping and filtering on the performance of OFDM," *IEEE Commun. Lett.*, vol. 2, no. 5, pp. 131–133, May 1998.
[13] A. Wilkinson and A. E. Jones, "Minimization of the peak to mean envelope power ratio of multicarrier transmission schemes by block coding," in *Proc. IEEE VTC*, vol. 2, July 1995, pp. 825–829.
[14] S. H. Müller, R. W. Bäuml, R. F. H. Fischer, and J. B. Huber, "OFDM with reduced peak-to-average power ratio by multiple signal representation," *Annuals Telecommun.*, vol. 52, no. 1, pp. 58–67, 1997.
[15] R. W. Bauml, R. F. H. Fischer, and J. B. Huber, "Reducing the peak-to-average power ratio of multicarrier modulation by selected mapping," *IEEE Electron. Lett.*, vol. 32, no. 22, pp. 2056–2057, Oct. 1996.
[16] B.-J. Choi, E.-L. Kuan, and L. Hanzo, "Crest-factors study of MC-CDMA and OFDM," in *Proc. IEEE VTC*, May 1999, pp. 233–237.
[17] L. J. Cimini Jr. and N. R. Sollenberge, "Peak-to-average power ratio reduction of an OFDM signal using partial transmit sequences," *IEEE Commun. Lett.*, vol. 4, pp. 86–88, Feb. 2000.
[18] T. Wada, T. Yamazato, M. Katayama, and A. Ogawa, "A Constant amplitude coding for orthogonal multicode CDMA systems," *IEICE Trans. Fund.*, vol. E80-A, pp. 2477–2484, Dec. 1997.
[19] Z. Bai, and K. Kwak, "A novel M-ary code-selected direct sequence BPAM UWB communication system," *ETRI J.*, vol. 28, no. 1, pp. 95–98, Feb. 2006.
[20] S. P. Kim and M. J. Kim, "Constant amplitude coding for code select CDMA system," in *Proc. IEEE TENCON*, vol. 2, Oct. 2002, pp. 1035–1038.
[21] J. G. Proakis, *Digital Communications*, 3th Ed. New York: McGraw-Hill, 1995.
[22] M.-S. Alouini and A. J. Goldsmith, "A unified approach for calculation error rates of linearly modulated signals over generalized fading channels," *IEEE Trans, Commun.*, vol. 47, pp. 1324–1334, Sept. 1999.

Kwanwoong Ryu was born in Deagu, Korea, on July 30, 1972. He received the B.S. and M.S. degrees in Electronics Engineering and the Ph.D. degree in Information and Communication Engineering from Yeungnam University, Korea, in 1997, 1999, and 2006, respectively. From February 2004 to January 2005, he was an internship student in the IP Radio Network Development Department of NTT DoCoMo, Inc. in Japan. In 2006, he joined a Senior Staff Engineer in XRONet Corporation. His research interests are multicarrier systems, and MIMO mode selection and intercell interference cancellation in Wibro System. He was awarded the Headong Best Paper Award from Korean Institute of Communication Sciences in 2005.

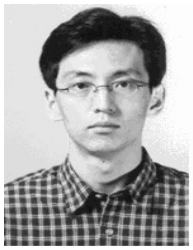

Jiyu Jin received his M.S. and Ph.D. degrees in Information and Communication Engineering from Yeungnam University, in 2003 and 2007, respectively. From April 2007 to February 2008, he was a Post Doctoral Researcher in the School of Electrical Engineering and Computer Science, Seoul National University. He is currently an Assistant Professor of Information and Communication Engineering at Yeungnam University. His research interests are in the areas of MIMO and multicarrier systems.

Youngwan Park received the B.E. and M.E. degrees in Electrical Engineering from Kyungpook National University, Daegu Korea, in 1982 and 1984, respectively, and his M.S. and Ph.D. degrees in Electrical Engineering from State University of New York at Buffalo, U.S.A. in 1989 and 1992, respectively. He joined the California Institute of Technology as a Research Fellow from 1992 to 1993. From 1994 to 1996, he has served as a Chief Researcher for developing IMT-2000 system at SK Telecom, Korea. Since September 1996, he has been a Professor of Information and Communication Engineering at Yeungnam University, Korea. From January to February of 2000, he was an Invited Professor at NTT Mobile Communications Network Inc. (NTT DoCoMo) Wireless Lab, Japan. He was also a Visiting Professor at UC Irvine, U.S.A, in 2003. Currently, he is serving as a Director of Technology Innovation Center for wireless multimedia by Korean government. From 2008 to 2009, he also serves as the President of IEEE VTS Seoul Chapter. His current research areas of interest includes Beyond 3G/4G system, OFDM system, PAPR reduction, LBS in wireless communication, etc.

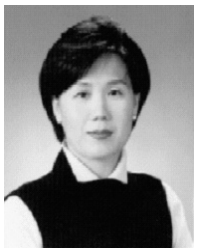

Jeong-Hee Choi received the B.S. degree from Kyungpook National University, Korea, in 1986. And she received M.S. and Ph.D. degrees in Electrical and Computer Engineering from State University of New York at Buffalo in 1989 and 1992, respectively. From 1994 to 1998, she was a Senior Researcher at SK Telecom Central Research Center, Korea. She is currently an Associate Professor in the School of Computer and Communication Engineering at Daegu University, Korea. Her research interests are raw data/signal processing of synthetic aperture radar imaging system and terrestrial/satellite mobile communication system.